Semicond. Sci. Technol. **26** (2011) 085003 (9pp) doi:10.1088/0268-1242/26/8/085003

Electrical characteristics of Mo/4H-SiC Schottky diodes having ion-implanted guard rings: temperature and implant-dose dependence

A Latreche[1], Z Ouennoughi[1,4], A Sellai[2], R Weiss[3] and H Ryssel[3]

[1] Laboratoire optoélectronique et composants, Département de physique, UFAS, Sétif, Algeria
[2] Physics Department, PO Box 36, Sultan Qaboos University 123, Oman
[3] FIIS, Schottkystrasse 10, 91058 Erlangen, Germany

E-mail: ouennoughi@gmail.com

Received 2 January 2011, in final form 1 March 2011
Published 26 April 2011
Online at stacks.iop.org/SST/26/085003

Abstract

The electrical characteristics of ion-implanted guard rings for molybdenum (Mo) Schottky diodes on 4H-SiC are analyzed on the basis of the standard thermionic emission model and the assumption of a Gaussian distribution of the barrier height. For edge termination, high-resistivity guard rings manufactured by carbon and aluminum ion-implanted areas were used. Extractions of barrier heights of molybdenum on silicon carbide (4H-SiC) Schottky diodes have been performed on structures with various gate metallization, using both current–voltage–temperature (*I–V–T*) and capacitance–voltage (*C–V*) measurements. Characteristic features of the Schottky barrier height (SBH) are considered in relation to the specific dose of the carbon- or aluminum-implanted guard ring. Contacts showed excellent Schottky behavior ideality factors between 1.02 and 1.24 in the range of 303–473 K. The measured SBHs were between 0.92 and 1.17 eV in the same temperature range from *I–V–T* characteristics. The variations in the barrier height, which is significantly temperature- and implantation-dose-dependent, are well fitted to a single Gaussian distribution function. Experimental results agree reasonably well by using this approach, particularly for carbon implantation dose of 1.75×10^{14} cm^{-2}, and a mean barrier height ($\bar{\Phi}_{B0}$) of 1.22 eV and zero bias standard deviation $\sigma_0 = 0.067$ V have been obtained. Furthermore, the modified Richardson plot according to the Gaussian distribution model resulted in a mean barrier height ($\bar{\Phi}_{B0}$) and a Richardson constant (A^*) of 1.22 eV and 148 A cm^{-2} K^{-2}, respectively. The A^* value obtained from this plot is in very close agreement with the theoretical value of 146 A cm^{-2} K^{-2} for n-type 4H-SiC. Therefore, it has been concluded that the temperature dependence of the forward (*I–V*) characteristics of the Mo/4H-SiC contacts can be successfully explained on the basis of a thermionic emission conduction mechanism with Guassianly distributed barriers.

1. Introduction

Silicon carbide is a wide band gap semiconductor that is of particular interest for applications in high-power and high-temperature electronics. Remarkable advances have been accomplished in SiC power semiconductor devices in recent years [1–3] with two key aspects being the focus of much of the research efforts. The first concerns the properties of the metal-SiC contacts, of either ohmic or rectifying nature, which are an essential part of any device and are, as such, of paramount fundamental and technological importance [4–12]. The second aspect is related to improvements in

[4] Author to whom any correspondence should be addressed.

the reverse voltage breakdown and the blocking properties of the SiC power devices, where it is necessary to reduce field enhancement at the edge of the device. Within the latter context, various techniques such as field plates [13], guard rings [8, 14], junction termination extension [15] or multistep junction termination extension [16] have been suggested to attain high breakdown voltages. The formation of guard rings for 4H-SiC Schottky diodes by carbon (C) and aluminum (Al) implantation have been reported in a previous publication [8] in which we have examined the effect of ion implantation-induced high-resistivity guard-ring structures on the behavior of the Schottky diodes. In the present contribution, we report the results of further studies of the electrical behavior of Mo/4H-SiC Schottky diodes. In particular, *I–V–T* and *C–V* measurements are used to ascertain the significant parameters and some of the salient features in direct relation to the current transport across the Mo/4H-SiC rectifying contacts. The effective Schottky barrier heights (SBHs) and ideality factors have been determined from the experimental forward bias *I–V–T* and reverse bias *C–V* characteristics of these diodes following analyses based on a modified thermionic emission theory. The effect of temperature and especially the impact of carbon or aluminum implantation doses on these parameters are reported. The electrical characteristics are discussed in the framework of the existing model of inhomogeneous barriers proposed by Werener and Guttler [17] with the assumption of a Gaussian lateral distribution of the SBH as suggested by the linear relationship between experimental effective BHs and ideality factors. When Schottky barrier parameters are re-evaluated using this model instead of the pure thermionic emission model, values of the barrier height and effective Richardson constant that are more reliable and much more consistent with previously published data on Mo/4H-SiC diodes [18–21] are obtained.

2. Device fabrication and characterization

Molybdenum Schottky diodes with high-resistivity guard rings were manufactured on an n-type 4H-SiC (0 0 0 1) substrate with the Si-face 8° off-oriented toward $\langle 1\,1\,\bar{2}\,0\rangle$. The wafers had an n-type epitaxial layer with a donor concentration in the range of 8.0×10^{15}–1.3×10^{16} cm^{-3}. The high-resistivity layer forming the guard ring was generated by carbon and aluminum ion implantation using a Varian 350 D ion implanter. The ion implantation was performed at room temperature and at different energies and doses ranging from 1.2×10^{12} to 1.75×10^{14} cm^{-2} for carbon, and from 1×10^{14} cm^{-2} to 9×10^{14} cm^{-2} for aluminum. The Schottky contacts, with a circular geometry, were formed by e-beam evaporation of Mo on the SiC substrate at a pressure of approximately 1×10^{-5} Pa followed by annealing in an open furnace at 500 °C under a N_2 flow of about 1000 sccm. A detailed description of the fabrication steps of these Schottky diodes was given previously [8, 22]. The *I–V* measurements were performed using a Keithley 237 source and measurement unit, which is capable of handling voltages up to 1100 V. The electrical *I–V–T* measurements of the Schottky diodes were made in the temperature range of 303–473 K with a step of 25 K. It has to be noted that in our *I–V–T* measurements, the typical reading error in the current is less than 1% and the temperature is determined with accuracy better than 0.1 K. The *C–V* measurements were conducted using an HP 4284A LCR meter at the frequency of 1 MHz at ambient temperature.

3. Results and discussion

Figures 1(*a*) and (*b*) show the measured forward *J–V–T* characteristics of the Mo/4H-SiC Schottky diodes with carbon terminated contacts (denoted as C_TC diodes with area = 7.07×10^{-4} cm^2) and with aluminum terminated contacts (denoted Al_TC with area = 1.76×10^{-4} cm^2), respectively. All Schottky contacts exhibited a similar forward *I–V* characteristics behavior with a wide linear region that extends over several orders of magnitudes. However, for higher implantation doses, a significant reduction in the saturation current is observed. The *J–V* curves of figure 2 are those of the diodes with C-implanted guard rings for different ion implantation doses. This figure suggests at first sight that there is a correlation between the carbon dose implantation and the SBH. The same behavior has been obtained for Al_TC. To quantitatively analyze our *I–V–T* data, we consider, as a starting point, the thermionic emission–diffusion (TED) theory which we will later modify to account for departures from the ideal behaviour and include the lateral and Gaussian distribution of the non-homogeneous barrier.

To recapitulate briefly, the current through a homogeneous SBD at a forward bias V is described within the TED theory by [23]

$$I = I_s\left[\exp\left(\frac{\beta}{n}(V - R_s I)\right) - 1\right] \tag{1}$$

with the saturation current I_s defined by

$$I_s = AA^*T^2\exp(-\beta\Phi_{B0}) \tag{2}$$

where $\beta = q/kT$ is the inverse thermal voltage, A is the diode area, k is the Boltzmann constant, A^* is the modified Richardson constant and T is the temperature.

Starting from these basic equations, a computer program based on the method developed by Osvald and Dobrocka [24] is used to extract the parameters of the SBDs, namely the zero-bias SBH, the ideality factor (n) and the series resistance (R_s) associated with the bulk material in the semiconductor and the back ohmic contact. In the process of these extractions, the theoretical value of the Richardson constant (A^*), for 4H-SiC, was taken as equal to 146 A cm^{-2} K^{-2} [25]. It has to be noted in this respect that there is a wealth of methods that can be used to extract the ideality factor in a diode or a solar cell [26–28]. These methods have their advantages as well as their limits. The method we have used follows a generalized approach in extracting parameters such as the barrier height, ideality factor and the series resistance by considering the whole range of the experimental data (forward and reverse parts of the *I–V* curve). It uses a least-squares method that unambiguously allows the determination of these parameters with good accuracy; it works even in the absence of a linear part in the *I–V* curve and in situations where other currents such as

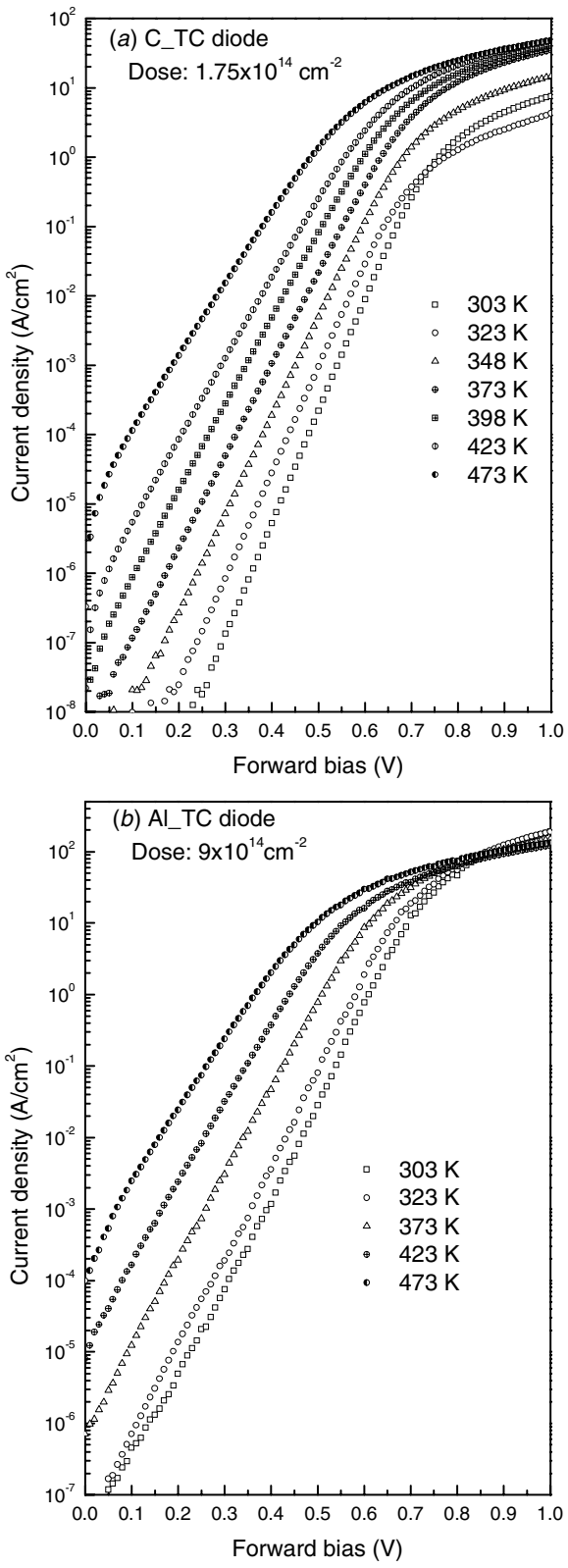

Figure 1. Forward experimental *J–V–T* curves of Mo/4H-SiC diode at different temperatures. (*a*) Carbon terminated (C_TC) diode, area = 7.07×10^{-4} cm^2, dose 1.75×10^{14} cm^{-2}. (*b*) Aluminum terminated (Al_TC) diode, area = 1.76×10^{-4} cm^2, dose = 9×10^{14} cm^{-2}.

leakage, thermionic field emission, generation-recombination currents are present at low forward and/or reverse bias.

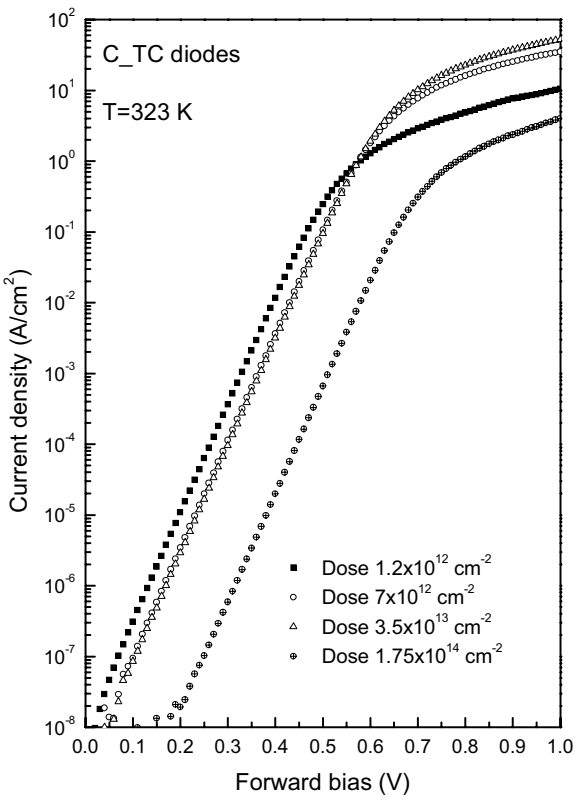

Figure 2. Forward experimental *J–V* curves of Mo/4H-SiC diode at different doses of carbon at 323 K.

Figure 3 shows that the barrier height and the ideality factor, for a given implantation dose, are manifestly temperature-dependent especially for the Al_TC diodes. The values of the SBHs and the ideality factor for the C_TC diodes range from 1.13 eV and 1.05 (at 303 K) to 1.17 eV and 1.02 (at 473 K), respectively, while those for Al_TC diodes extend from 0.92 eV and 1.25 (at 303 K) to 1.05 eV and 1.05 (at 473 K), respectively.

The barrier heights show generally a consistent increase with temperature, while the ideality factors (n) follow a temperature-dependent behavior and this is particularly manifest for Al_TC Schottky diodes, which is well in line with the typical behavior commonly referred to in the literature as the 'T_0' anomaly [29].

In figure 4, the extracted SBHs in the case of the C_TC diodes at different temperatures and for various implantation doses are shown. It is clear from this figure that the SBH increases with increasing doses of ion implantation.

Alternatively, rewriting equation (2) under the form

$$\ln(I_s/T^2) = \ln(AA^*) - (q/kT)\Phi_{B0} \tag{3}$$

allows the determination of both the SBH and the Richardson constant from respectively the slope and the intercept of the $\ln(I_s/T^2)$ versus $1/kT$ plot. These plots yielded an activation energy of 0.9 eV at lower doses (1.2×10^{12} cm^{-2}) and 1.08 eV at higher doses (1.75×10^{14} cm^{-2}) for C_TC diodes (0.77 eV for Al_CT at higher doses). The obtained Richardson constants were comprised between 13.71 A cm^{-2} K^{-2} for the lowest dose and 17.96 A cm^{-2} K^{-2} for the highest dose in

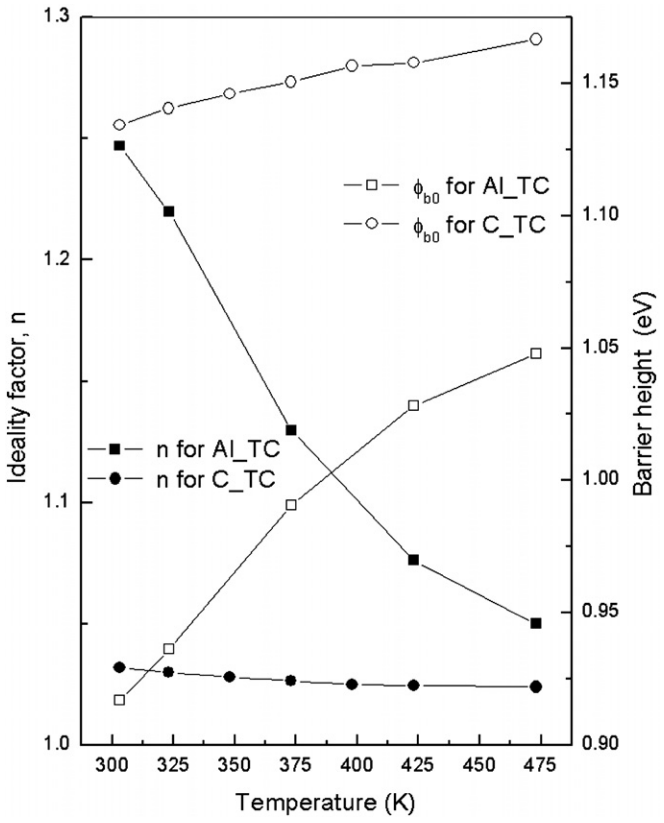

Figure 3. Ideality factor and SBH as a function of the absolute temperature for Mo/4H-SiC diodes with carbon dose of 1.75 × 10^{14} cm^{-2} and aluminum dose of 9 × 10^{14} cm^{-2}.

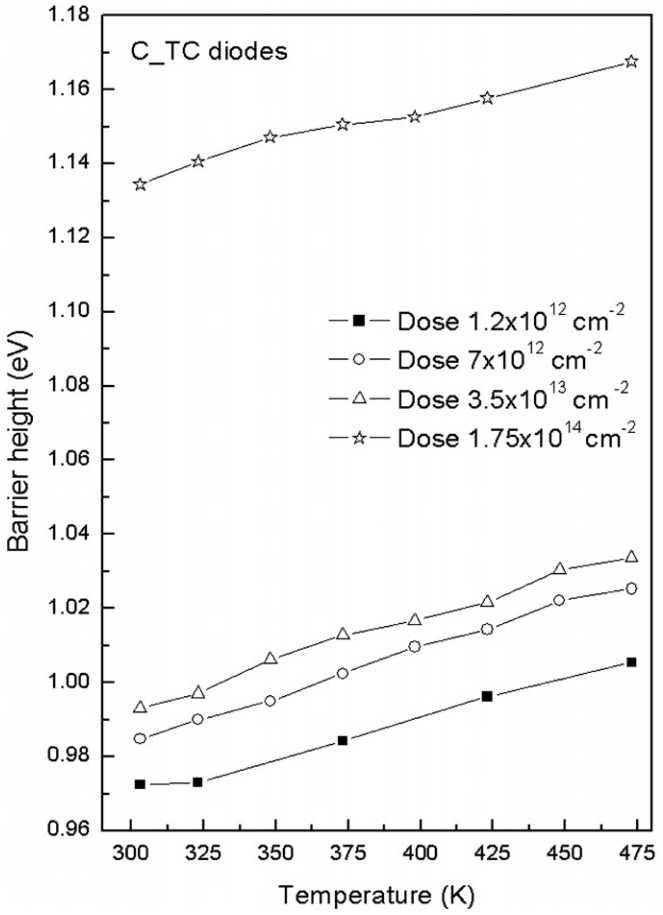

Figure 4. Extracted SBH of C_TC diodes at different temperatures for different doses.

the case C_TC diodes, while it was only 0.16 A cm^{-2} K^{-2} for Al_CT at the higher dose. The Richardson constant values are, in all instances, much lower than the known theoretical value of 146 A cm^{-2} K^{-2}. The discrepancy between experimental and calculated Richardson constants could be, as explained below, due to the spatial inhomogeneities of the BHs [9].

The analyses developed around the T_0-parameter are essentially empirical approaches to linearize the Richardson plots but do not have a physical meaning. A more physical approach is to interpret the departure from ideal thermionic emission by considering the inhomogeneity of the barrier when the combined effects of image force lowering, field emission tunneling and recombination processes are not enough to account for the measured fluctuations in the barrier height. It is well established through direct imaging using ballistic electron emission microscopy (BEEM) studies that Schottky potential barriers of a number of systems are generally not homogeneous but may consist of patches of relatively lower or higher barriers with respect to a mean value. This suggested that thermionic emission theory should be modified to include this spatial distribution in the barrier to adequately analyze the electrical characteristics of Schottky diodes. One of the features of such an approach is that the current flow would be substantially influenced by regions of lower barrier height at low temperatures.

Of course, there are a number of physical reasons to which the inhomogenities at a metal–semiconductor contact can be ascribed. These include doping inhomogeneity, contamination at the interface causing high interface state density, native defects, and a mixture of different phases [6, 17, 30]. And it is true that in most Schottky contacts, a model based on the pure thermionic emission theory fails to describe the measured current–voltage characteristics. Hence, to explain experimental observations and anomalies, inhomogeneity models which assume a spatial and statistical variation [17, 31] of the barrier height across the junction can be applied to describe the non-ideal Schottky junctions. Moreover, figure 1(*a*) shows crossover between the 303 and 323 K characteristics also observed in figure 1(*b*). This crossing is generally explained by the existence of the Gaussian distribution of barrier heights in inhomogeneous Schottky diodes [32, 33]. The analytical model of the Gaussian distribution of barrier heights favors this crossing [32].

In this context and as a further step in our analyses, with the aim of remedying to the departures from the non-ideal behavior highlighted above, the forward *I–V* characteristics are analyzed on the basis of a modified thermionic emission model that incorporates the spatial variation of the barrier height. The barrier distribution is supposed to be Gaussian [17, 31, 34] with a mean value ($\bar{\Phi}_B$), a standard deviation (σ) and of the form

$$P(\Phi_B) = \frac{1}{\sigma\sqrt{2\pi}} \exp\left[-\frac{(\Phi_B - \overline{\Phi}_B)^2}{2\sigma^2}\right]. \qquad (4)$$

Table 1. The extracted mean barrier heights $\overline{\Phi}_{B0}$ and zero-bias standard deviation σ_0 for C_TC diodes at various doses.

Dose (cm^{-2})	$\overline{\Phi}_{B0}$(eV)	σ_0 (V)
1.2×10^{12}	1.08	0.078
7×10^{12}	1.10	0.079
3.5×10^{13}	1.11	0.080
1.75×10^{14}	1.22	0.067

The total *I–V* across a Schottky diode containing barrier inhomogeneities can be expressed as

$$I(V) = \int_{-\infty}^{\infty} \mathrm{i}(V, \Phi_B) \mathrm{P}(\Phi_B) \mathrm{d}\Phi_B \tag{5}$$

where $\mathrm{i}(V,\Phi_B)$ is the elementary current at a bias V for a barrier of height (Φ_B), given by equation (1) and $P(\Phi_B)$ is the normalized distribution function giving the probability of the occurrence of the barrier height (Φ_B).

Assuming a linear bias dependence of $\bar{\Phi}_B$ and a quadratic bias dependence of σ such as $\overline{\Phi}_B - \overline{\Phi}_{B0} = \rho_2 V$ and $\sigma^2 - \sigma_0^2 = \rho_3 V$ and performing integration of equation (5), one can obtain the current *I–V* through a Schottky barrier at a forward bias *V*:

$$I = I_s' \left[\exp\left(\frac{\beta}{n_{\mathrm{ap}}} (V - R_s I) \right) - 1 \right] \tag{6}$$

with

$$I_s' = A A^{**} T^2 \exp(-\beta \Phi_{\mathrm{ap}}). \tag{7}$$

Equations (6) and (7) are similar to equations (1) and (2) except that Φ_{B0} and n are replaced by Φ_{ap} and n_{ap}, which are respectively the apparent barrier height and apparent ideality factor. These are given by

$$\Phi_{\mathrm{ap}} = \overline{\Phi}_{B0} - \frac{\beta \sigma_0^2}{2} \tag{8}$$

and

$$\frac{1}{n_{\mathrm{ap}}} = 1 - \rho_2 + \frac{\beta \rho_3}{2} \tag{9}$$

where σ_0 is the standard deviation at zero bias. The coefficients ρ_2 and ρ_3 are independent of temperature and quantify the voltage deformation of the barrier distribution.

The very good linearity of the Φ_{ap} versus $1/2\ kT$ plot (figure 5) is clear evidence of the Gaussian distribution of the barrier height. The mean barrier height ($\bar{\Phi}_{B0}$) and the zero-bias standard deviation (σ_0) can be obtained from this plot. Table 1 gives the extracted values of $\bar{\Phi}_{B0}$ and σ_0 for C_TC samples, from which it is clear that the mean barrier height increases with increasing carbon dose implantation.

The same behavior has been observed for the Al_TC diodes, i.e. the mean barrier increases with the Al implantation dose. For an implantation dose of 9×10^{14} cm^{-2}, the Al-implanted Mo-Schottky diode showed a mean barrier height of 1.29 eV, which is significantly larger than the mean barrier height for the C_TC diodes at a comparable carbon implantation dose of 1.75×10^{14} cm^{-2}.

It has to be noted that the carbon dose must be multiplied by a factor of 0.25 to take into account the lower nuclear stopping cross-sections (compared to Al) and to allow for the comparison of both implantation doses [8].

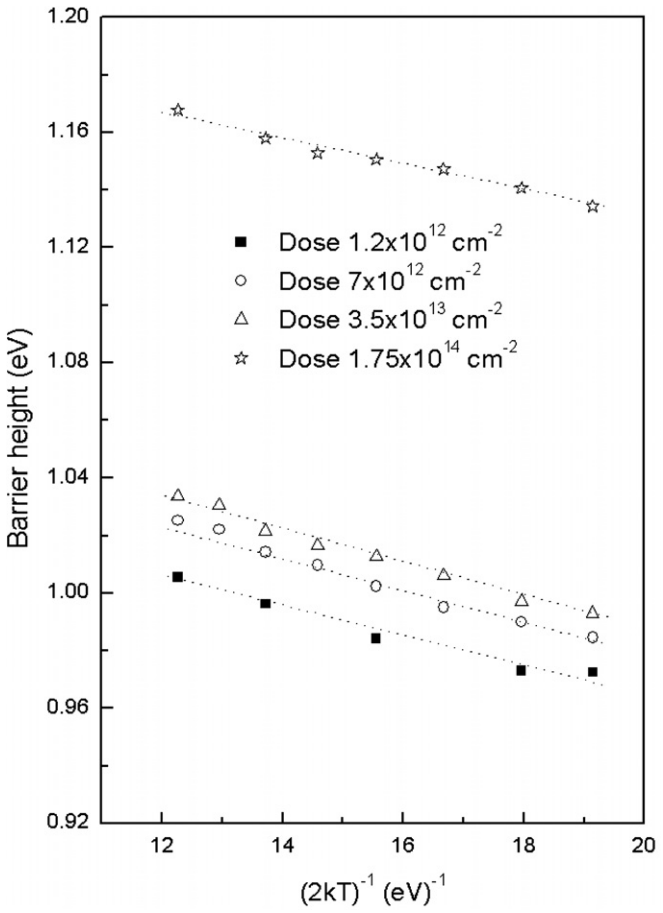

Figure 5. Apparent barrier height versus $1/2\ kT$ curve of C_TC diodes at various doses according to the Gaussian distribution.

The temperature dependence of the ideality factor can be understood on the basis of equation (9), which indicates that the $1/n_{\mathrm{ap}}$ versus $1/2\ kT$ plot should give a straight line (as shown in figure 6) the slope and intercept of which give the voltage coefficients ρ_3 and ρ_2, respectively. Values of $\rho_2 = -0.238$ and $\rho_3 = -22.9$ mV were obtained for Al_TC diodes, while values of $\rho_2 = -0.0051$ and $\rho_3 = -1.34$ mV were recorded for the case of C_TC diodes. The values obtained for ρ_2 and ρ_3 are of the same order of magnitude, particularly for the Al_TC diodes case, as those published previously in the literature [35–37].

The Richardson constants, which were shown to deviate substantially from the calculated value of 146 A cm^{-2} K^{-2}, were re-derived from a modified Richardson plot that takes into account the Gaussian distribution of the barrier:

$$\ln\left(\frac{I_s}{T^2}\right) - \left(\frac{q^2\sigma_o^2}{2k^2T^2}\right) = \ln\left(AA^*\right) - \frac{q\overline{\Phi}_{B0}}{kT}. \tag{10}$$

The $\ln(I_s/T^2)$-$(q^2{\sigma_0}^2)/2\ k^2T^2$ versus $1/(kT)$ plot according to equation (10) should also be a straight line with the slope and the intercept at the ordinate directly yielding the mean barrier height $\bar{\Phi}_{B0}$ and A^*, respectively. Figure 7 depicts this plot which clearly exhibits excellent linearity over the whole temperature range with corresponding activation energies of

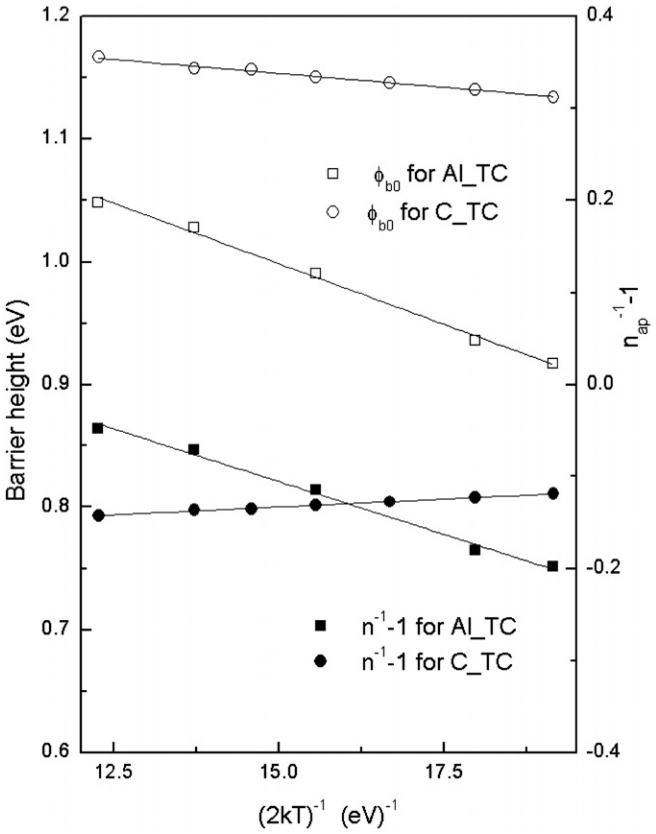

Figure 6. Zero bias apparent barrier height and $(1/n_{ap}-1)$ versus $1/2\ kT$ plot of Mo/4H-SiC diodes according to the Gaussian distribution with carbon dose of 1.75×10^{14} cm^{-2} and aluminum dose of 9×10^{14} cm^{-2}.

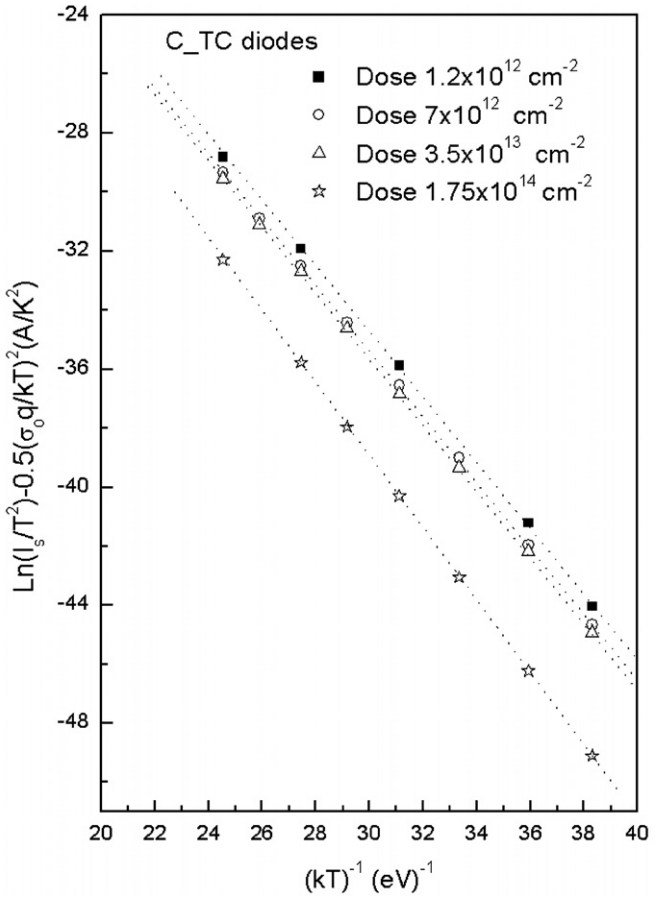

Figure 7. Modified Richardson plot $\ln(I_s/T^2)$-$(q^2\sigma_0{}^2)/2\ k^2T^2$ versus $1/(kT)$ of C_TC diodes according to the Gaussian distribution at various doses.

the order of $\bar{\Phi}_{B0}$. Using a linear least-squares fitting procedure of the data of the C_TC diodes at an implantation dose of 1.75×10^{14} cm^{-2}, $\bar{\Phi}_{B0}$ and A^* were obtained to be 1.22 eV and $A^* = 148$ A cm^{-2} K^{-2}, respectively. The values of A^* and $\bar{\Phi}_{B0}$ obtained from the modified Richardson plot were 128 A cm^{-2} K^{-2} and 1.28 eV respectively, for the Al_TC diode.

It has to be noted that the derived value of $\bar{\Phi}_{B0}$ is practically the same as the one obtained above from the apparent barrier plot of figure 6. What is more remarkable, however, is that the A^* values (148 and 128 A cm^{-2} K^{-2}) obtained from these modified plots are by far in much better agreement with the theoretical value of 146 A cm^{-2} K^{-2} for n-type 4H-SiC.

The results of the capacitance–voltage measurements performed at room temperature and at 1 MHz in the case of C_TC diodes with various dose implantations are presented in figure 8. An absence of hysteresis has been observed via room temperature capacitance–voltage (C–V) measurements in which the voltage bias was scanned both in the increasing and decreasing directions.

Capacitance–voltage data were used to extract the SBHs and doping by fitting a straight line to $C^{-2}(V)$ plotted

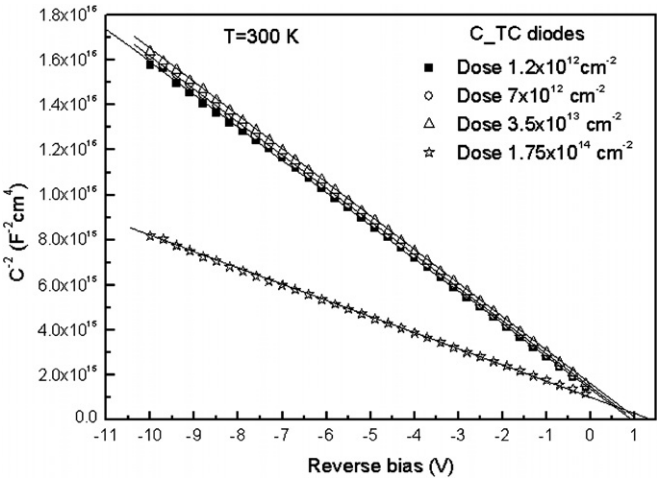

Figure 8. Experimental reverse bias $C^{-2}(V)$ characteristics of Mo/4H-SiC Schottky diodes at various carbon doses at 300 K.

as a function of the reverse voltage, using the standard equation [23]

$$C^{-2} = \frac{2}{A^2 q N_D \varepsilon_s}(V_i - V) \tag{11}$$

where A is the diode area, N_D is the net donor concentration, ε_s is the static dielectric constant of the semiconductor, and

Table 2. The extracted barrier heights (Φ_{B0}^{CV}, Φ_{B0}^{IV}) and doping concentrations N_D for C_TC diodes at 300 K.

Dose (cm^{-2})	Φ_{B0}^{CV} (eV)	Φ_{B0}^{IV} (eV)	N_D (cm^{-3})
1.2×10^{12}	1.04	0.97	9.57×10^{15}
7×10^{12}	1.05	0.98	9.51×10^{15}
3.5×10^{13}	1.12	0.99	9.44×10^{15}
1.75×10^{14}	1.57	1.13	1.98×10^{16}

V_i is the intercept along the voltage axis, which relates to the SBH by

$$\Phi_{B0}^{CV} = V_i + \xi + kT/q \tag{12}$$

where ξ is the energy difference between the Fermi level and the bottom of the conduction band. (denotes the semiconductor level Fermi level with respect to E_c) and $\xi = \frac{kT}{q} \ln\left(N_C / N_D\right)$ depends on the effective density of states N_C in the conduction band and on the doping which is deducible from the slope of the $C^{-2}(V)$ plot. The experimental values of Φ_{B0}^{CV} and N_D determined using the experimental data in conjunction with equations (11) and (12) are summarized in table 2 for each dose.

Table 2 reveals a significant difference between the barriers Φ_{B0}^{CV} and Φ_{B0}^{IV}, which are derived from capacitance–voltage (C–V) and current–voltage (I–V) measurements, particularly at higher doses. The values of N_D obtained from the slope of the $C^{-2}(V)$ plots are very close to the doping densities of wafers as supplied by the manufacturer.

Note that the C–V characteristics are usually affected by the presence of a thin interfacial oxide-like layer between the Schottky metal and the semiconductor. The real bias voltage applied to the depletion layer deviates from the measured voltage and is usually lower. Hence, V_i, the intercept voltage in the $C^{-2}(V)$ plot, was estimated to be larger than the real value.

There are further considerations that should be highlighted with respect to the results presented above. Although it was not possible for us to put directly into evidence the barrier inhomogeneities using a technique such as ballistic electron emission spectroscopy (BEEM), it is clear from our analysis that the state of the metal/SiC interface is ultimately responsible for the underestimation of the value of A^* when inhomogeneities were not considered. In fact, it is known that molybdenum can readily react with the SiC to form a silicide, when reacted with elemental Si and form carbide when reacted with elemental C, and show little added reaction when performing an annealing up to 800 °C [38]. The evidence thus indicates that reactions and the creation of new phases (Mo_2C, $MoSi_2$, Mo_3Si) can increase the barrier height and lead to significant inhomogeneity due to a mixture of different phases at the M–S interface. This is besides the fact that SiC may contain structural and morphological defects that have been identified as micropipes, screw dislocations, grain boundaries, triangular depressions and growth pits. These defects were shown to exist both in the substrates and overgrown epilayers [3]. Identification of defects in SiC, their densities and ways to reduce them is a very active area of research at present.

A number of publications have reported the use of molybdenum (Mo) for fabrication of high-performance Schottky devices. Using C–V measurements, Yakimova *et al* [5] reported SBHs of the order of 1.03 and 1.28 eV. Nakamura *et al* [18] prepared SBDs using Mo contacts followed by annealing at a high temperature, derived a barrier height of 1.2–1.3 eV from I–V measurements and reported no degradation in the ideality factor or in the reverse characteristics. Similarly, Mo/4H-SiC diodes fabricated by Vassilevski *et al* [19] revealed the unchanging ideality factor and barrier height (1.21–1.3 eV) at the temperature up to 400 °C. Shigilshoff *et al* reported the SBH of 1.3 eV derived from I–V measurements and 1.66 eV derived from the C–V measurement for Mo/4H-SiC (Si-face). Recently, Mo Schottky contacts have been characterized by Perrone *et al* [21] and the contacts show a SBH of 1.04–1.08 eV from electrical measurements.

From these cited works, the SBHs obtained for the same metal under different experimental conditions are significantly different. This difference can be attributed to the different conditions of preparation of the devices, i.e. the quality of the semiconductor, surface preparation, the morphology of the surface, the edge of termination used and also the temperature of annealing. However, the homogeneous SBH value obtained using a Gaussian distribution model, in this work, is very close to the theoretical SBH $\Phi_B = \Phi_m - \chi$ of about 1.23 eV expected for the Mo/4H-SiC SBH obtained by considering the molybdenum work function, $\Phi_m = 4.53$ eV, and the usually used value of the electron affinity of 4H-SiC, $\chi = 3.3$ eV. Note that the work function of a metal can be anisotropic. Generally, the relationship $\Phi_B = S(\Phi_m - \chi) + (1 - S)(E_g - \Phi_0)$, where E_g is the energy gap, Φ_0 the pinning level due to interface states and S the index of interfacial behavior, is commonly used to interpret measurements on Schottky barriers and SiC is an intermediate case [10] between $S = 0$ and $S = 1$. Also the approach used in this paper (Gaussian distribution) does not consider the lateral length scale of the inhomogeneity and the pinch-off effect related to the interaction between adjacent regions with different barriers as suggested by Tung [39].

SBDs usually exhibit low SBH and hence leakage current higher than that predicted by the conventional thermionic emission theory. In general, SiC high-voltage SBDs utilize edge termination in order to minimize surface leakage current and prevent breakdown at the device edge.

For high-voltage Schottky diodes, it is necessary to have an edge termination around the periphery of the diodes to reduce the electric field crowding at the diode edges [13]. As mentioned above, several techniques have been shown to reduce the field crowding at the edges, thus resulting in higher breakdown voltages. Ion implantation is the most used method to locally modify the electrical properties of SiC-based devices [40].

The edge termination for high-voltage SiC Schottky diodes reported so far in the literature has been achieved mostly by Ar, B or Al implantation [19, 20, 41–43]. In most of these studies, ion implantation results in the creation of a resistive, amorphous layer which allows the potential to

spread across the surface of the biased sample, increasing the breakdown voltage. The electrical properties of SiC material and SiC devices have been shown to change significantly due to ion implantation and particularly, aluminum implantation leads to surface roughness which increases with Al concentration [44]. Unfortunately, their correlations to the implantation conditions are not clear and merit additional consideration.

The presented results support the conclusion that the Al-implanted Schottky diodes with an active guard-ring structure had the highest SBH and obviously show the lowest leakage current as was observed by Weiss *et al* [8] when they investigated the effect of ion-implanted high-resistivity guard-ring structures on the behavior of Mo, W and Ni Schottky diodes.

4. Conclusion

Mo Schottky contacts to n-type 4H-SiC with guard-ring structures were characterized, and the results of electrical measurements on the devices are presented along with the SBH and ideality factor. Furthermore, two different samples having different edge termination were investigated. The barrier heights obtained from the current–voltage (*I–V*) measurements on both samples are essentially identical, with an average value of a mean barrier height of 1.22 eV. The current–voltage (*I–V*) measurements on the Mo Schottky devices yielded barrier heights that were much smaller than those obtained from the capacitance–voltage (*C–V*) measurements.

The extracted SBHs Φ_{B0} are dependent on the dose of implantation of the guard ring and were in the range of 0.92–1.17 eV which are in good agreement with previously published data on Mo/4H-SiC Schottky diodes.

The experimental data were described by an inhomogeneous model which takes into account the fluctuation of the surface potential and this procedure, in turn, enabled the correct determination of the Richardson constant, in satisfying agreement with the theoretical value.

Based on information gained from SiC defect investigation and various accomplishments published by other researchers, the more plausible causes of these inhomgeneities may be indicated in the presence of surface defects in the material and/or interface roughness. A microstructural analysis of the Mo–SiC interface would be necessary to correlate electrical behaviors with ion implantation doses.

References

[1] Baliga J 2005 *Silicon Carbide Power Devices* (Singapore: World Scientific)

[2] Shur M, Rumyantsev S and Levinshtein M 2006 *SiC Materials and Devices* (Singapore: World Scientific)

[3] Park Y S 1998 *SiC Materials and Devices, Semiconductors and Semimetals* ed R K Willardson and E R Weber (San Diego, CA: Academic)

[4] Itoh A and Matsunami H 1997 *Phys. Status Solidi* a **162** 389–408

[5] Yakimova R, Hemmingsson C, Macmillan M F, Yakimov T and Janzén E 1998 *J. Electron. Mater.* **27** 871–5

[6] Defives D, Noblanc O, Dua C, Brylinski C, Bartula M, Aubry-Fortuna V and Meyer F 1999 *IEEE Trans. Electron Devices* **46** 449–55

[7] Skromme B J, Luckowski E, Moore K, Bhatnagar M, Weitzel C E, Gehoski T and Ganser D 2000 *J. Electron. Mater.* **29** 376–83

[8] Weiss R, Frey L and Ryssel H 2001 *Appl. Surf. Sci.* **184** 413–8

[9] Roccaforte F, La Via F, Raineri V, Pierobon R and Zanoni E 2003 *J. Appl. Phys.* **93** 9137–44

[10] Shigiltchoff O, Bai S, Devaty R P, Choyke W J, Kimoto T, Hobgood D, Neudeck P G and Porter L M 2003 *Mater. Sci. Forum* **433–436** 705–8

[11] Pérez R, Mestres N, Montserrat J, Tournier D and Godignon P 2005 *Phys. Status Solidi* a **202** 692–7

[12] Pirri C F, Ferrero S, Scaltrito L, Perrone D, Guastella S, Furno M, Richieri G and Merlin L 2006 *Microelectron. Eng.* **83** 86–8

[13] Saxena V, Su J N and Steckl A J 1999 *IEEE Trans. Electron Devices* **46** 456–63

[14] Ueno K, Urushidani T, Hashimoto K and Seki Y 1995 Al/Ti Schottky barrier diodes with the guard-ring termination for 6H–SiC *Proc. Int. Symp. Power Semiconductor Devices and ICs* 107–11

[15] Sheridan D C, Niu G and Cressler J D 2001 *Solid-State Electron.* **45** 1659–64

[16] Alexandrov P, Wright W, Pan M, Weiner M, Jiao L and Zhao J H 2003 *Solid-State Electron.* **74** 263–9

[17] Werner J H and Güttler H H 1991 *J. Appl. Phys.* **69** 1522–33

[18] Nakamura T, Miyanagi T, Kamata I, Jikimoto T and Tsuchida H 2005 *IEEE Electron Device Lett.* **26** 99–101

[19] Vassilevski A *et al* 2006 *Mater. Sci. Forum* **237–529** 931–4

[20] Vassilevski A, Nakamura T, Horsfall A, Wright N G, O'Neill A G, Hilton K P, Munday A G, Hydes A J, Uren M J and Johnson C M 2007 *Mater. Sci. Forum* **556–557** 873–6

[21] Perrone D, Naretto M, Ferrero S, Scaltrito L and Pirri C F 2009 *Mater. Sci. Forum* **615–617** 647–50

[22] Toumi S, Ferhat-Hamida A, Boussouar L, Sellai A, Ouennoughi Z and Ryssel H 2009 *Microelectron. Eng.* **86** 303–9

[23] Rhoderick E H and Williams R H 1988 *Metal-Semiconductor Contacts* 2nd edn (Oxford: Clarendon)

[24] Osvald J and Dobrock E 1996 *Semicond. Sci. Technol.* **11** 1198–202

[25] Bozack M J 1997 *Phys. Status Solidi* **b 2002** 549–77

[26] Jain A and Kapoor A 2005 *Sol. Energy Mater. Sol. Cells* **85** 391–6

[27] Kavasoglu N, Kavasoglu A S and Oktik S 2009 *Curr. Appl. Phys.* **9** 833–8

[28] Singh N S, Jain A and Kapoor A 2009 *Sol. Energy Mater. Sol. Cells* **93** 1423–6

[29] Saxena A N 1969 *Surf. Sci.* **13** 151–71

[30] Sullivan J P, Tung R T, Pinto M R and Graham W R 1991 *J. Appl. Phys.* **70** 7403–24

[31] Song Y P, Van Meirhaeghe R L, Laflère W H and Cardon F 1986 *Solid-State Electron.* **29** 633–8

[32] Chand S 2004 *Semicond. Sci. Technol.* **19** 82–6

[33] Osvald J 2006 *Solid-State Electron.* **50** 228–31

[34] Chand S and Kumar J 1996 *J. Appl. Phys.* **80** 288–94

[35] Bluet J M, Ziane D, Guillot G, Tournier D, Brosselard P, Montserrat J and Godignon P 2006 *Superlatt. Microstruct.* **40** 399–404

[36] Sefaoğlu A, Duman S, Doğan S, Gürbulak B, Tüzemen S and Türüt A 2008 *Microelectron. Eng.* **85** 631–5

[37] Aydin M E, Yildirim N and Türüt A 2007 *J. Appl. Phys.* **102** 043701–7

[38] Geib K M, Wilson C, Long R G and Wilmsen C W 1990 *J. Appl. Phys.* **68** 2796–800
[39] Tung R T 1992 *Phys. Rev.* B **45** 13509–23
[40] Giannazzo F, Roccaforte F and Raineri V 2007 *Appl. Phys. Lett.* **91** 202104
[41] Alok D and Baliga J 1997 *IEEE Trans. Electron Devices* **44** 1013–7
[42] Ivanov P A, Grekhov I V, Potapov A S and Samsonova T P 2008 *Semiconductors* **72** 858–61
[43] Roccaforte F, Giannazzo F, Iucolano F, Eriksson J, Weng M H and Raineri V 2010 *Appl. Surf. Sci.* **256** 5727–35
[44] Rambach M, Bauer A J and Ryssel H 2008 *Phys. Status Solidi* **b 245** 1315–26